Tikrit Journal of Pure Science Vol. 31 (2) 2026

DOI:https://doi.org/10.25130/tjps.v31i2.1960

IRAQI Academic Scientific Journals

Tikrit Journal of Pure Science

ISSN: 1813–1662 (Print) --- E-ISSN: 2415–1726 (Online)

Journal Homepage: https://tjpsj.org/

Tikrit Journal of Pure Science

Simulating the Effect of Temperature Change on the Properties of a Quantum Dot Solar Cell

Raed Khaleel Zahoo[1], Q. N. Abdullah[2]

[1,2]Department of Physics, College of Education for Pure Sciences, University of Tikrit, Tikrit, Iraq

Received: 23 Mar. 2025 **Received in revised forum:** 5 May 2025 **Accepted:** 11 May 2025

Final Proofreading: 15 Apr. 2026 **Available online:** 25 Apr. 2026

ABSTRACT

To develop solar cell technology, it is essential to focus on improving its efficiency at the temperatures typically encountered during operation. This study used third-generation quantum-dot solar cells (ITO/NiO/GaAs/CdTe/ZnO/Al). These cells exhibit electrical and optical properties suitable for photovoltaic applications. The impact of temperature on the performance of quantum dot solar cells is simulated using Silvaco Atlas, a tool for simulating experimental solar cells. The temperature in this work ranged from (300 K) to (350 K). The results confirmed a decrease in the solar cell's overall photovoltaic performance with increasing temperature. The electricity conversion performance decreased from (11 %) to (9.36 %), and the fill component reduced from (81.06 %) to (78.14 %). The open-circuit voltage also decreased from 0.98 V to 0.87 V. The short-circuit current density decreases slightly from (13.839 mA/cm^2) to (13.7642 mA/cm^2) with increasing temperature. The maximum energy of the solar cell also decreased from (2.2×10^{-11}W) to (1.87×10^{-11} W) with growing temperature. This study revealed that the optimal temperature for the solar cell is 300 K, i.e., room temperature.

Keywords: Gallium arsenide, Quantum dot solar cell, Silvaco Atlas, Temperature

Name: Raed Khaleel Zahoo **E-mail: Ar230074ued@st.tu.edu.iq**

Tikrit Journal of Pure Science Vol. 31 (2) 2026
DOI:https://doi.org/10.25130/tjps.v31i2.1960

محاكاة تأثير تغير درجة الحرارة على خصائص الخلية الشمسية ذات النقاط الكمية

رائد خليل زهو[1]، قحطان نوفان عبد الله[2]

[1,2]قسم الفيزياء، كلية التربية للعلوم الصرفة، جامعة تكريت، تكريت، العراق

الملخص

لتطوير تقنية الخلايا الشمسية، من الضروري التركيز على تحسين كفاءتها في درجات الحرارة التي تواجهها عادةً أثناء التشغيل. استُخدمت في هذه الدراسة خلايا شمسية من الجيل الثالث بتقنية النقاط الكمومية (ITO/NiO/GaAs/CdTe/ZnO/Al). تُظهر هذه الخلايا خصائص كهربائية وبصرية مناسبة للاستجابة الكهروضوئية. تمت محاكاة تأثير درجة الحرارة على خصائص خلايا النقاط الكمومية الشمسية باستخدام برنامج سيلفاكو اطلس والذي يحاكي الواقع التجريبي للخلايا الشمسية. تراوحت درجة الحرارة في هذا العمل بين (300 K) و(350 K). أظهرت النتائج انخفاضًا في الأداء الكهروضوئي للخلية الشمسية مع زيادة درجة الحرارة. انخفضت كفاءة تحويل الطاقة من (11 %) إلى (9.36 %)، وانخفض عامل الملء من (81.06 %) إلى (78.14 %). كما انخفض جهد الدائرة المفتوحة من (0.98 V) إلى (0.87 V)، بينما لم يتأثر تيار الدائرة القصيرة تقريبًا بدرجة الحرارة. انخفضت القدرة القصوى للخلية الشمسية أيضًا من (2.2×10^{-11} W) إلى (1.87×10^{-11} W) مع ارتفاع درجة الحرارة. وكشفت هذه الدراسة أن درجة الحرارة المثلى للخلية الشمسية هي (300 K)، وهي درجة حرارة الغرفة.

INTRODUCTION

Solar power is crucial for advancing sustainable development. and decreasing dependence on traditional power assets [(1)]. To build a low-carbon economy, the best approach to addressing electricity and environmental issues is to use solar energy to generate electricity. Many types of solar cells have been investigated and developed, including Si solar cells, copper indium gallium selenide (CIGS) solar cells, and cadmium telluride (CdTe) solar cells. All of them have certain limitations that cannot be ignored, such as high fabrication costs and significant pollution, which limit their further applications. [(2)]. Over the last few decades, solar cells have evolved significantly, and they are categorized into three generations. Monocrystalline and polycrystalline silicon solar cells are first-generation solar cells. To address the high costs associated with first-generation solar cells that rely on expensive silicon materials, second-generation solar cells were developed using thin-film technology. Building on this advancement, third-generation solar cells were later introduced, offering not only lower costs but also improved efficiency across various types of solar cells. [(3)]. Quantum dot solar cells (QDSCs) show significant potential as an advanced photovoltaic technology. [(4, 5)]. Colloidal quantum dots (CQDs) are nanocrystals with dimensions smaller than the Bohr exciton radius. [(6, 7)]. Commonly used quantum dots include cadmium selenide (CdSe), cadmium telluride (CdTe), cadmium sulfide (CdS), and lead sulfide (PbS). One of the unique properties of quantum dots is their tunable band gap, which can be adjusted by simply varying their size. [(8)]. Due to this property of CQDs, there is an increase in the power conversion efficiency and performance of the CQDSCs [(9)]. To better utilize the solar cell spectrum, the tunable band gap of CQDs enables absorption of infrared radiation. Therefore, it becomes a promising candidate for tandem solar cell devices. [(10)].

The proposed solar cell structure comprises the absorber material GaAs, which absorbs light, nickel oxide (NiO) as a hole-transporting layer, and ZnO as an electron-transporting layer. In this work, we use the 2D atlas in Silvaco TCAD as a simulation, where it can calculate the properties of I-V and its photoelectric parameters, the most important of which are the open-circuit voltage (Voc), short-

circuit current density (Jsc), fill factor (FF), efficiency (η), and P-V properties. The default lighting spectrum is set to the international AM1.5 standard.

DEVICE STRUCTURE

The photovoltaic device used in this work is ITO/NiO/GaAs/CdTe/ZnO/Al as shown in Figure (1), which contains an indium tin oxide (ITO) layer as the front contact, NiO layer as the hole transport layer (HTL), a gallium arsenide (GaAs) absorber layer, CdTe quantum dot consists of (10 layers), each layer consists of (10 quantum dots), and the dimensions of one dot are (5×10 nm), ZnO as the electron transport layer (ETL), and aluminum (Al) as the back contact.

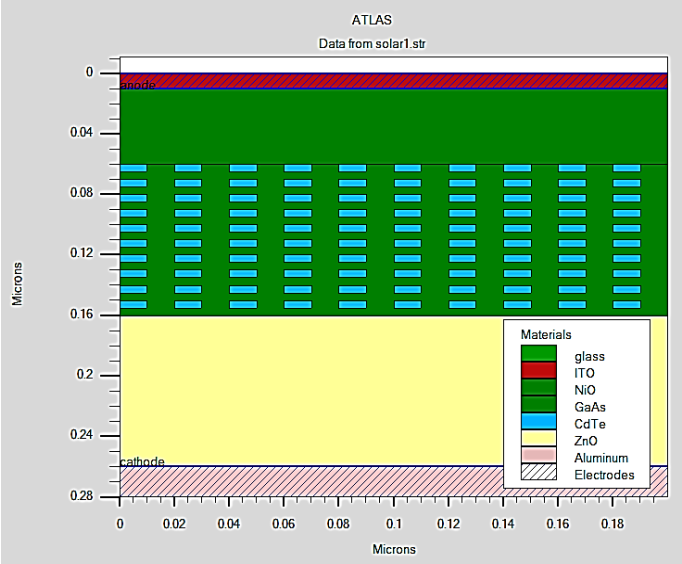

Fig. 1: Structure of a quantum dot solar cell.

THEORY APPROACH

The diffusion-drift transport model effectively describes the behavior of charge carriers under the influence of light or an electric field, leading to deviations from thermal equilibrium. This version focuses on solving a set of fundamental equations that underpin the ideal behavior of semiconductor devices, including solar cells.

Poisson's equation describes the relationship between potential and charge density and is given by:

$$\nabla \cdot \xi = \nabla^2 \varphi = \frac{\rho}{\varepsilon} \quad \ldots (1)$$

Since ξ is the permittivity of the material, and φ is the relationship that gives the potential, the charge density ρ in semiconductor devices:

$$\rho = q(p - n + N_D^+ - N_A^-) \quad \ldots (2)$$

In this context, (n) and (p) constitute the electron and hollow densities, while N_D^+ and N_A^- denote the densities of donor and acceptor ions, respectively [(11)].

Continuity equations relate the current density to the rate of generation and recombination of charge carriers. Furthermore, they take into account the law of charge conservation. Under steady-state conditions, the continuity equations for the electron and hole can be defined as:

$$\frac{1}{q} \nabla . J_n = R_n - G_n \quad \ldots (3)$$

$$\frac{1}{q} \nabla . J_p = -(R_p - G_p) \quad \ldots (4)$$

In this context, G denotes the optical generation rate of electron-hole pairs, and R represents the recombination rate of electrons and holes for the doped semiconductor. [(12)].

Electric current flow fundamentally arises from the movement of electrons and holes, facilitated by two primary transport mechanisms: drift and diffusion. Drift refers to the movement that results when an electric field (ξ) is applied across a semiconductor, whereas diffusion is driven by a concentration gradient [(13).] Consequently, the overall current

densities for electrons and holes are expressed as J_n and J_p, respectively, where:

$$J_n = q\mu_n n \xi + qD_n \nabla_n \quad \dots (5)$$

$$J_p = q\mu_p p \xi - qD_p \nabla_p \quad \dots (6)$$

Where μ_n and μ_p refer to the mobilities of electrons and holes, respectively, and D_n and D_p denote the diffusion coefficients for electrons and holes. In equations (5) and (6), the initial terms correspond to the drift currents, whereas the subsequent terms account for the diffusion currents. [14]. Table 1 presents the physical parameters obtained from published research and used in the simulation process in Silvaco Atlas Tcad, an advanced TCAD (Technology Computer-Aided Design) tool used for the design and analysis of electronic and optoelectronic devices at the nanoscale. The program enables users to simulate the performance and design of semiconductor devices, such as transistors, solar cells, and diodes, using realistic mathematical and physical models.

Table 1: The physical parameters utilized in the simulation process.

Parameters	Symbol (unit)	p-NiO (HTL) [19]	n-ZnO (ETL) [17, 18]	i-GaAs (active-layer) [16 ,15]
thickness	W (nm)	50	100	100
Band gap	E_g (eV)	3.5	3.3	1.42
Electron affinity	χ (eV)	2.2	4	4.07
Dielectric permittivity	ε_r	9	8.5	12.9
CB effective density of states	$N_C(cm^{-3})$	3×10^{19}	4×10^{18}	4.7×10^{17}
VB effective density of states	$N_V(cm^{-3})$	1.8×10^{19}	1.8×10^{19}	9×10^{18}
Electron thermal velocity	V_n(cm/s)	10^7	10^7	10^7
Hole thermal velocity)	V_P(cm/s)	10^7	10^7	10^7
Electron mobility	$\mu_e(cm^2/Vs)$	12	100	8500
Hole mobility	$\mu_h(cm^2/Vs)$	5	30	400
Shallow uniform donor density	ND (cm^{-3})	0	1×10^{18}	$1x\ 10^{15}$
Shallow uniform acceptor density	NA (cm^{-3})	1×10^{18}	0	0
Electron lifetime (Taun)	τ_n	1×10^{-5}	1×10^{-5}	5.1×10^{-7}
hole lifetime (Taup)	τ_p	1×10^{-5}	1×10^{-5}	5.1×10^{-7}

RESULTS AND DISCUSSION

Raising the temperature of a solar cell can diminish its performance, leading to decreased production capacity and efficiency. Higher temperatures affect the properties of semiconductor materials, resulting in a narrowing of the semiconductor's bandgap. [20]. The increased energy of electrons in the material may be the reason for the narrowing of the bandgap with increasing temperature. As a result, the energy required to break the bond decreases. This section presents the temperature-dependent performance of the solar cell device while holding all other parameters constant. Figure 2 shows the current-voltage curve of the solar cell as the temperature changes from 300 K to 350 K. All electrical and optical properties are held constant during the simulation. As the temperature increases, the reverse saturation current increases, which decreases the open-circuit voltage due to its temperature sensitivity. The lower V_{OC} makes it easier for the electrons to gain sufficient energy at higher temperatures and recombine with the holes. [21, 22].

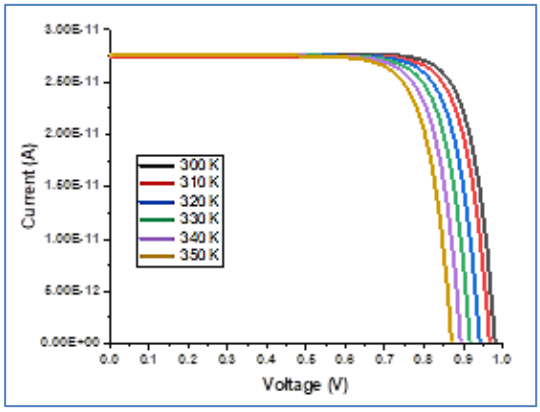

Fig. 2: The current-voltage characteristic curve of the quantum dot solar cell with temperature change.

Table 2 highlights the key performance metrics of a quantum dot (QD) solar cell: open-circuit voltage (Voc), short-circuit current density (Jsc), fill factor (FF), and power conversion efficiency (PCE) as the temperature shifts from 300 K to 350 K. This data is used to understand the thermal behavior of a 10-layer quantum dot solar cell. With rising temperatures, all device parameters show a decline. [23]. The short-circuit current density decreases slightly from (13.839 mA/cm^2) to (13.7642 mA/cm^2) with increasing temperature due to the increase in reverse saturation current with increasing temperature of the solar cell. The open-circuit voltage decreases significantly, from 0.98 V to 0.87 V, as the temperature increases. This reduction in Voc occurs because higher temperatures narrow the material's band gap. [24]. Table 2 also shows that the solar conversion efficiency decreased from (11 %) to (9.36 %). The fill factor (FF) value also decreased from (81 %) to (78 %) due to increased thermal recombination and internal resistance of the cell. Therefore, to achieve optimal performance, the solar cell temperature should be (300 K).

Table 2: Properties of the (quantum dot solar cell) with temperature change.

Temperature (K)	Voc (V)	Jsc (mA/cm^2)	FF (%)	PCE (%)
300	0.98	13.839	81.06	11
310	0.96	13.7644	80.40	10.69
320	0.94	13.76435	79.93	10.36
330	0.917	13.7643	79.40	10.02
340	0.89	13.76425	78.81	9.69
350	0.87	13.7642	78.14	9.35

Figure 3 shows the power-voltage curve of a solar cell with temperature changes. The electrical power of the solar cell decreases from (2.2 × 10^{-11} W) to (1.87 × 10^{-11} W) as the temperature increases from (300 K) to (350 K). This decrease in power is mainly due to the decrease in the open-circuit voltage [25].

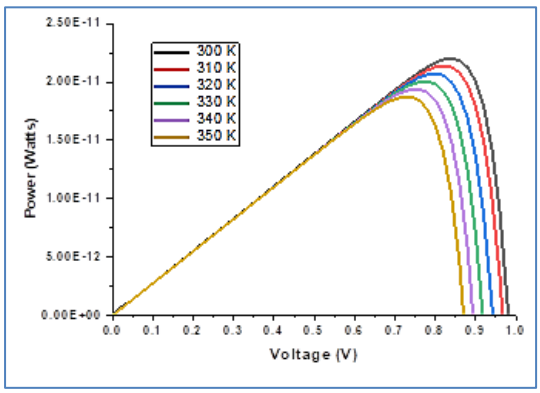

Fig. 3: Power-voltage characteristic curve of the quantum dot solar cell with temperature change.

CONCLUSION

With continuous advances in solar-to-electricity conversion technologies, quantum dot solar cells have emerged as among the most promising technologies for achieving high efficiency at low cost. In this study, the Silvaco ATLAS simulation software was used to optimize the overall performance of an ITO/NiO/GaAs/CdTe/ZnO/Al quantum dot solar cell. During the simulation, all optical and electrical properties were held constant to observe the effects of temperature changes on the solar cell. A decrease in the overall cell performance was observed as the temperature increased from 300 K to 350 K. The best results were achieved at 300K, with a conversion efficiency of (11 %), a fill factor of (81.06 %), a short-circuit current density of (13.839 mA/cm^2) and an open-circuit voltage of

(0.98 V). We also obtained a maximum solar cell power of (2.2 × 10^{-11} W). For future studies, it is necessary to select a suitable operating temperature for the solar cell to achieve high efficiency.

Conflict of interests: The authors declare that there is no conflict of interest regarding the publication of this paper.

Sources of funding: This research did not receive any specific grant from funding agencies in the public, commercial, or not-for-profit sectors.

Author contributions: The authors contributed equally to the study.

REFERENCES

1. Mahmood YH, Atallah FS, Youssef AF. Studying the weather conditions affecting solar panel efficiency. Tikrit Journal of Pure Science. 2020;25(3):98-102. https://doi.org/10.25130/tjps.v25i3.255

2. Shwan YH, Ghafoor BN. Study the Effect of Doping and Thickness on IV characteristics of Silicon Solar Cells Using PC1D Simulation. Tikrit Journal of Pure Science. 2024;29(1):128-35. https://doi.org/10.25130/TJPS.V29I1.1520

3. Salim KD. Studying the effect of light intensity and the dust on the efficiency of a Silicon Solar cell. Tikrit Journal of Pure Science. 2021;26(4):68-70. https://doi.org/10.25130/tjps.v26i4.164

4. Tong Y, Xiao Z, Du X, Zuo C, Li Y, Lv M, et al. Progress of the key materials for organic solar cells. Science China Chemistry. 2020;63:758-65. https://doi.org/10.1007/s11426-020-9726-0

5. Sahu A, Garg A, Dixit A. A review of quantum dot-sensitized solar cells: Past, present and future toward carrier multiplication and the possibility of higher efficiency. Solar Energy. 2020;203:210-39. https://doi.org/10.1016/j.solener.2020.04.044

6. Zhou R, Niu H, Ji F, Wan L, Mao X, Guo H, et al. Band-structure tailoring and surface passivation for highly efficient near-infrared responsive PbS quantum dot photovoltaics. Journal of Power Sources. 2016;333:107-17. https://doi.org/10.1016/j.jpowsour.2016.09.160

7. Fukuda T, Takahashi A, Takahira K, Wang H, Kubo T, Segawa H. Limiting factor of performance for solution-phase ligand-exchanged PbS quantum dot solar cell. Solar Energy Materials and Solar Cells. 2019;195:220-7. https://doi.org/10.1016/j.solmat.2019.03.011

8. Song JH, Jeong S. Colloidal quantum dot-based solar cells: from materials to devices. Nano Convergence. 2017;4:1-8. https://doi.org/10.1186/s40580-017-0115-0

9. Song X, Ma Z, Li L, Tian T, Yan Y, Su J, et al. Aqueous synthesis of alloyed CdSexTe1-x colloidal quantum dots and their In-situ assembly within mesoporous TiO2 for solar cells. Solar Energy. 2020;196:513-20. https://doi.org/10.1016/j.solener.2019.12.049

10. Kim J, Ouellette O, Voznyy O, Wei M, Choi J, Choi MJ, et al. Butylamine-catalyzed synthesis of nanocrystal inks enables efficient infrared CQD solar cells. Advanced Materials. 2018;30(45):1803830. https://doi.org/10.1002/adma.201803830

11. Guerra N, Guevara M, Palacios C, Crupi F. Operation and physics of photovoltaic solar cells: an overview. I+D Tecnológico. 2018;14(2):84-95. https://doi.org/10.33412/idt.v14.2.2077

12. Babu P, Padmanabhan T, Ahamed M, Sivaranjani A. Studies on copper indium selenide/Zinc sulphide semiconductor quantum dots for solar cell applications. Chalcogenide Letters. 2021;18(11). https://doi.org/10.15251/CL.2021.1811.701

13. Vitanov S, Palankovski V, Maroldt S, Quay R. High-temperature modeling of algan/gan hemts. Solid-State Electronics. 2010;54(10):1105-12. https://doi.org/10.1016/j.sse.2010.05.026

14. Aissat A, Boubakeur M, Benyettou F, Vilcot JP, éditeurs. Optimization of Structure InAsxSb1-xL GaAs Quantum Dot Solar Cell. 2017 International Renewable and Sustainable Energy Conference (IRSEC); 2017: IEEE. https://doi.org//10.1109/IRSEC.2017.8477379

15. Kilway RJ. Five-junction solar cell optimization using Silvaco ATLAS: Monterey, California: Naval Postgraduate School; 2017. https://doi.org/10.1016/j.nanoen.2023.108979

16. Ahmed IM, Alsaif OI, Algwari QT. The Effect of Quantum Dots on the Performance of the Solar Cell. Iraqi Journal for Electrical & Electronic Engineering. 2024;20(2).
https://doi.org/10.1016/j.solener.2019.10.009
17. Raoui Y, Ez-Zahraouy H, Tahiri N, El Bounagui O, Ahmad S, Kazim S. Performance analysis of MAPbI3-based perovskite solar cells employing diverse charge selective contacts: Simulation study. Solar Energy. 2019;193:948-55.
https://doi.org/10.1016/j.solener.2019.10.009
18. Al Husseini HB, Jafar AM. An analysis comparing the performance of lead and tin halides organic perovskite solar cells and numerical simulation with SCAPS. Optical Materials. 2024;155:115814.
https://doi.org/10.1109/ICIAS.2016.7824055
19. Campos T. Study of 2D/3D perovskites heterostructures for solar cells: Université Paris-Saclay; 2023.
https://doi.org/10.37917/ijeee.20.2.20
20. Li J, Wang H, Luo M, Tang J, Chen C, Liu W, et al. 10% Efficiency Cu2ZnSn (S, Se) 4 thin film solar cells fabricated by magnetron sputtering with enlarged depletion region width. Solar energy materials and solar cells. 2016;149:242-9.
https://doi.org/10.1016/j.solmat.2016.02.002
21. Lin P, Lin L, Yu J, Cheng S, Lu P, Zheng Q. Numerical simulation of Cu2ZnSnS4-based solar cells with In2S3 buffer layers by SCAPS-1D. Journal of Applied Science and Engineering. 2014;17(4):383-90.
https://doi.org/10.6180/jase.2014.17.4.05.
22. Tiwari R, Dubey P, Lohia P, Dwivedi D, Fouad H, Akhtar M. Simulation engineering in quantum dots for efficient photovoltaic solar cell using copper iodide as hole transport layer. Journal of Nanoelectronics and Optoelectronics. 2021;16(12):1897-904.
https://doi.org/10.1166/jno.2021.3143
23. Sullivan BP. The effect of temperature on the optimization of photovoltaic cells using Silvaco ATLAS modeling: Monterey, California. Naval Postgraduate School; 2010.
https://doi.org/10.4236/eng.2010.211112
24. Hamsa A. Performance Optimization of Cu (In1-x, Gax)(Se1-y, Sy) 2 Thin-Film Solar Cells by Characterization and Modeling of Temperature and Low-Light Behavior: Universität Oldenburg; 2021.
https://doi.org/10.1002/pip.2695.
25. Sharma P, Goyal P. Analyzing the effects of solar insolation and temperature on PV cell characteristics. Materials Today: Proceedings. 2021;45:5539-43.
https://doi.org/10.1016/j.matpr.2021.02.301